

# The MMT All-Sky Camera

T. E. Pickering<sup>a</sup>

<sup>a</sup>MMT Observatory, 933 N. Cherry Ave., Tucson, AZ 85721, USA;

## ABSTRACT

The MMT all-sky camera is a low-cost, wide-angle camera system that takes images of the sky every 10 seconds, day and night. It is based on an Adirondack Video Astronomy StellaCam II video camera and utilizes an auto-iris fish-eye lens to allow safe operation under all lighting conditions, even direct sunlight. This combined with the anti-blooming characteristics of the StellaCam's detector allows useful images to be obtained during sunny days as well as brightly moonlit nights. Under dark skies the system can detect stars as faint as 6th magnitude as well as very thin cirrus and low surface brightness zodiacal features such as gegenschein. The total hardware cost of the system was less than \$3500 including computer and framegrabber card, a fraction of the cost of comparable systems utilizing traditional CCD cameras.

**Keywords:** Sky Monitoring, All-Sky Imaging, Observatory Site Conditions

## 1. INTRODUCTION

“How clear is it?” is a question every astronomer asks while observing. It can often be answered by simply going outside and looking at the sky. However, the human eye takes several minutes to become fully dark-adapted so thin cloudiness can often be missed. Another common question that can be much harder to answer is “How clear was it when my data was taken?” Answering that requires some archived record of sky conditions that can be searched or queried.

Wide-angle imaging is a popular way of monitoring the sky that can provide a real-time view of current conditions. Images from such a system can also be analyzed quantitatively and archived for later use. One of the best-known examples of this is the Michigan Tech CONCAM<sup>1</sup> system. Other observatories have deployed their own all-sky imaging systems such as CASCA at Las Campanas (<http://ascam2.lco.cl/>), TASCA<sup>2</sup> at Cerro Tololo, SNOOP at Mt. Palomar (<http://snoop.palomar.caltech.edu/>), and ESO's MASCOT<sup>3</sup> at Cerro Paranal. These systems all use CCDs to obtain visual to near-IR images. It is also possible to detect clouds directly in the near to mid-IR using systems such as the one deployed at Apache Point.<sup>4</sup> IR-based systems have the advantage of detecting clouds equally well under all conditions (e.g. dark time vs. bright time). However, they require much more complicated and expensive optics and detectors. The Apache Point system, for example, cost in excess of \$100,000.

The MMT's budget was far more limited than that and even the \$20,000 that CONCAM quotes for one of their systems was well out of reach. We were not initially interested in that level of photometric and astrometric precision, anyway. We simply wanted something that could reliably go as deep visually as a dark-adapted human eye under dark skies while still providing useful images under a full moon.

## 2. CAMERA HARDWARE

The genesis of the idea of a low-cost video-based all-sky camera came about when testing some inexpensive low-light video cameras with wide-angle lenses. We discovered that if we fed the signal into a framegrabber card, integrated several seconds worth of frames, and subtracted a dark frame, we could detect stars down to 2nd or 3rd magnitude. A quick back-of-the-envelope calculation determined that a camera that did the integration internally could easily reach 5th or 6th magnitude, the naked eye limit. StellaCam video cameras from Adirondack Video Astronomy (AVA) perform just this kind of on-camera integration.

---

Author E-mail Address: [tpickering@mmto.org](mailto:tpickering@mmto.org)



**Figure 1.** Pictures of the installed sky camera system. The image on the left shows the enclosure and junction box mounted on a pole at the east end of the summit parking lot. The image on the right shows the entrance window of the enclosure.

We opted for the StellaCam II system because it provides the capability of full computer automation via an RS232 interface and can integrate for up to 256 frames (8.53 seconds). It used to be the case that high quality ultra-wide-angle “fish-eye” lenses were very expensive. However, it is now possible to find several reasonably good C/CS mount fish-eye lenses for under \$200 that provide a full 180° field-of-view. We went with a Fujinon YV2.2X1.4A-SA2 that is carried by AVA. Similar lenses are made by Pelco and others and sold by companies that specialize in CCTV hardware. Initial testing was performed with the manual-iris version of the lens, but we switched to the auto-iris version when it became available. The StellaCam II has an auto-iris port and testing showed that this combination could be safely used during the day under direct sunlight and thus allow full 24/7 operation.

The lack of a need for a mechanical shutter greatly simplifies the enclosure requirements. We decided to try an off-the-shelf outdoor security camera enclosure from Pelco, the EH2515. It’s compact, inexpensive, and fully sealed against rain and dust by tight O-ring seals. Our unit came with an optional heater/defroster unit that turned out to be defective. Fortunately, we have found that it has not really been necessary. The heat from the camera and its power supply are usually sufficient to keep the small enclosure warm enough to prevent condensation. The front of the fish-eye lens is set back about 1 cm from the lip of the enclosure. This cuts down the field-of-view slightly from a rated 185° to a measured 150°. Pointing a flat window straight up raised a few eyebrows at first, but it has worked out very well. The seal around the window has held up to numerous rain storms and has only needed occasional cleaning. The front of the enclosure does fill up like a bowl in heavy rain, but this does not affect the seal. In fact, this helps move dirt off the clear part of the window by wind blowing the water around and by the enclosure’s slight offset from vertical. The camera can still take clear pictures of the sky while the front is filled with water which was a little disconcerting when first observed. Pictures of the as-installed system can be seen in Figure 1.

### 3. COMPUTING AND SOFTWARE

Automating the camera system and digitizing its data requires a computer. For simplicity, we decided not to co-locate the computer with the camera. The threat of lightning on an exposed mountain peak like the MMTO site means that any connections between a computer and an instrument located outdoors need to be optically-isolated. Fiber optic modems for RS232 communication are common and relatively inexpensive, but we were unsure of how well we’d be able to transmit video over fiber. The Luxcom Technologies OM-7 was one of the least expensive alternatives we found that promised high video quality. In lab testing we found no measurable difference between images taken with and without the fiber link. The extra digitization step obviously must

degrade the signal somewhat, but in our case it is masked by noise and the 8-bit digitization of the framegrabber card. In fact, using two short lengths of coaxial cable plus the fiber link generates better image quality than using a single  $> 30$  meter coaxial cable that would otherwise be required.

The requirements for the computer that runs the system are fairly modest. It is currently a 2.4 GHz Celeron with 1 GB of RAM and a 160 GB hard drive. It is packaged into a small-form-factor case manufactured by Shuttle. Basically, the only strict requirements are a PCI slot for the framegrabber card and enough CPU and memory to generate a 100-image animation within a few seconds. The framegrabber card is an Integral Technologies FlashBus MV. It was chosen for its combination of low noise, good image quality, and linux-compatibility. It is color-capable, but can be configured to run in a lower-noise monochrome mode that we use.

Integral Technologies provides a SDK along with their linux device driver. It was used along with the CFITSIO<sup>5</sup> library to build some C programs to read and co-add images from the framegrabber and output the results in FITS format. The RS232 interface for the StellaCam comes only with software for Windows, but a description of the RS232 protocol was made available upon request. The protocol is implemented in the form of a script that takes the configuration parameters as arguments.

The system as a whole is managed by a single master script. Upon initialization, the script checks the time of day and times of sunrise and sunset, and configures the StellaCam accordingly to reasonable defaults. For safety, the StellaCam's auto-iris control is always enabled. There is no automatic gain control within the StellaCam system so the master script manages the gain and exposure settings by monitoring image statistics. If the images become too dark, the exposure time is increased until it reaches the 256 frame maximum. Then the gain is increased until the mean brightness of the image falls within the desired range. If the images become too bright, the gain is lowered until it reaches its minimum value and then the exposure time is stepped down. The maximum exposure time equates to about 8.5 seconds so images are acquired every 10 seconds. This allows sufficient time for post-processing of images and creating animations of the most recent 100 frames.

After the system was installed, the image coordinate system was calibrated by running the IRAF routine `daofind` on a set of images to generate lists of detected stars and matching those lists against known stars. The times of the exposures were used to generate altitude and azimuth coordinates for the stars. When building a transformation from polar ( $alt, az$ ) coordinates to cartesian ( $x, y$ ) image coordinates it is useful to define an intermediate set of polar coordinates in the image, ( $R, \theta$ ). Taking into account sign conventions and image origin, the transformation for ( $R, \theta$ )  $\rightarrow$  ( $x, y$ ) is:

$$\begin{aligned} x &= x_0 - R * \sin(\theta) \\ y &= y_0 + R * \cos(\theta) \end{aligned}$$

where ( $x_0, y_0$ ) is the position of zenith. We do not see any significant angular variation so the conversion from azimuth to  $\theta$  is straightforward:

$$\theta = Az + \theta_{\text{off}} \quad (1)$$

where  $\theta_{\text{off}}$  is simply a measure of the camera's rotation offset with respect to the sky.  $R$  corresponds to the zenith angle,  $z = 90 - Alt$ . To account for distortion in the lens, we use a 3rd order polynomial to model the transformation between  $z$  and  $R$ :

$$R = a * z + b * z^2 + c * z^3 \quad (2)$$

which leaves us a total of 6 unknowns to solve for. In the system's current configuration, these parameters are:

$$\begin{aligned} x_0 &= 298.861 \\ y_0 &= 228.746 \\ \theta_{\text{off}} &= 12.94^\circ \\ a &= 3.203 \text{ pixels}/\circ \\ b &= 2.46 \times 10^{-3} \text{ pixels}/\circ^2 \\ c &= -1.21 \times 10^{-4} \text{ pixels}/\circ^3 \end{aligned}$$

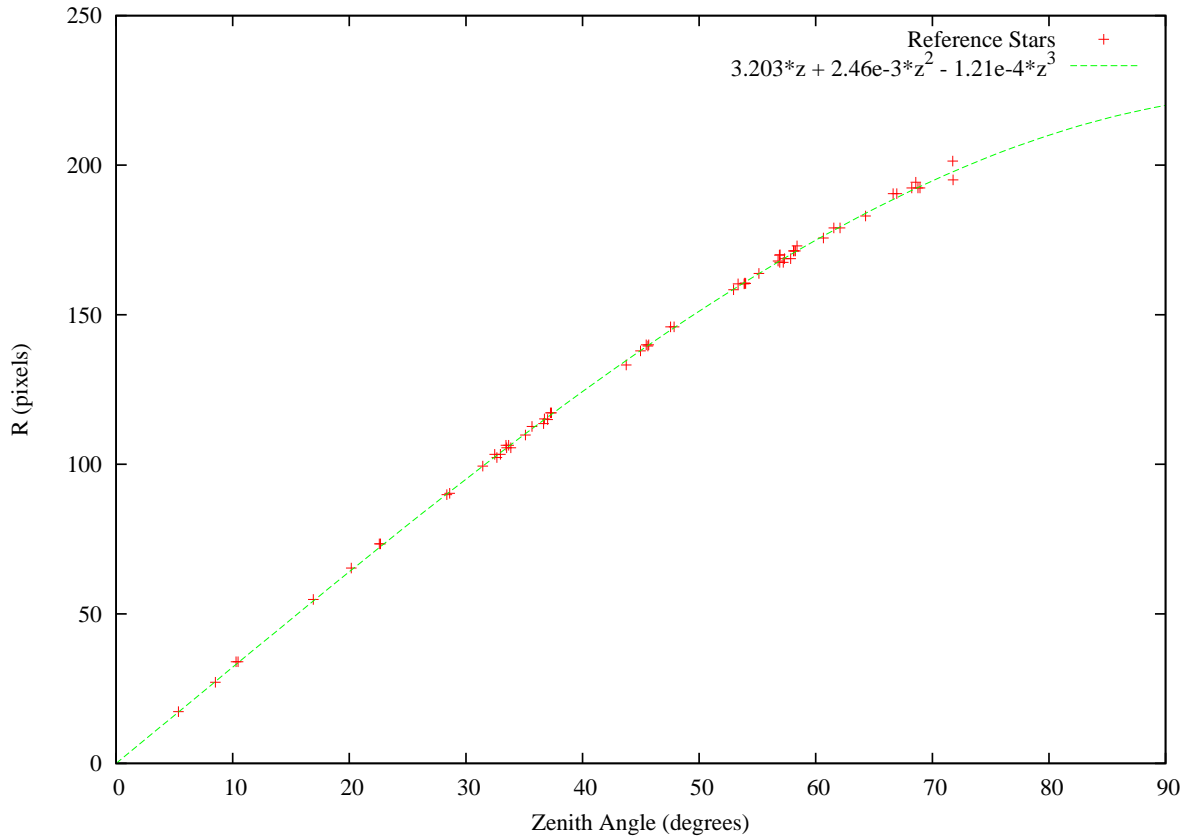


**Figure 2.** Radius,  $R$ , from zenith point in image versus zenith angle for a set of reference stars along with the best-fit polynomial transform.

Figure 2 shows some reference star data plotted along with the best-fit transform from  $z$  to  $R$ . These parameters need to be recalculated whenever the camera system is moved in any way, but have proven to be very stable over time when the system is left alone. The elevation cutoff due to the enclosure works out to be about  $15^\circ$ . The RMS scatter about the best-fit coordinate transform is 1.2 pixels.

#### 4. OPERATION AND PERFORMANCE

The performance of the system under dark skies exceeded our expectations. With an exposure time of 256 frames and the gain set to moderately high values ( $\sim 100$  out of 127) it can easily reach 5th magnitude and often fainter. What the camera sees is at least comparable to what a person can see when their eyes are fully adjusted for the dark. Figure 3 shows a representative example of an image obtained during a dark, clear night. The Milky Way is plainly visible rising in the east. The bright star nearly due south is Jupiter and the MMT building can be seen in the west. After an image is taken, the MMT's TCS is queried and a red cross placed in the image to denote where the MMT is pointing. Figure 4 shows a gallery of other interesting images taken under various conditions.

Images and animations from the all-sky camera are displayed and continuously updated on large monitors in the MMT control room. This provides observers and telescope operators instant appraisal of what the sky conditions are outside. The 100 frame ( $\sim 15$  minute) animations are especially useful for seeing cirrus and haze that might otherwise go unnoticed. The camera is sensitive enough to see gravito-acoustic waves in the airglow emission under certain conditions. They look like very light cirrus, but the animations show how they move



**Figure 3.** Representative image taken by the MMT All-Sky Camera on a clear, moonless night. The timestamp of the image and the camera configuration information are shown in the upper left corner of the image. The cardinal directions are plotted on the image for reference along with a red cross at the position that corresponds to where the MMT is pointing.

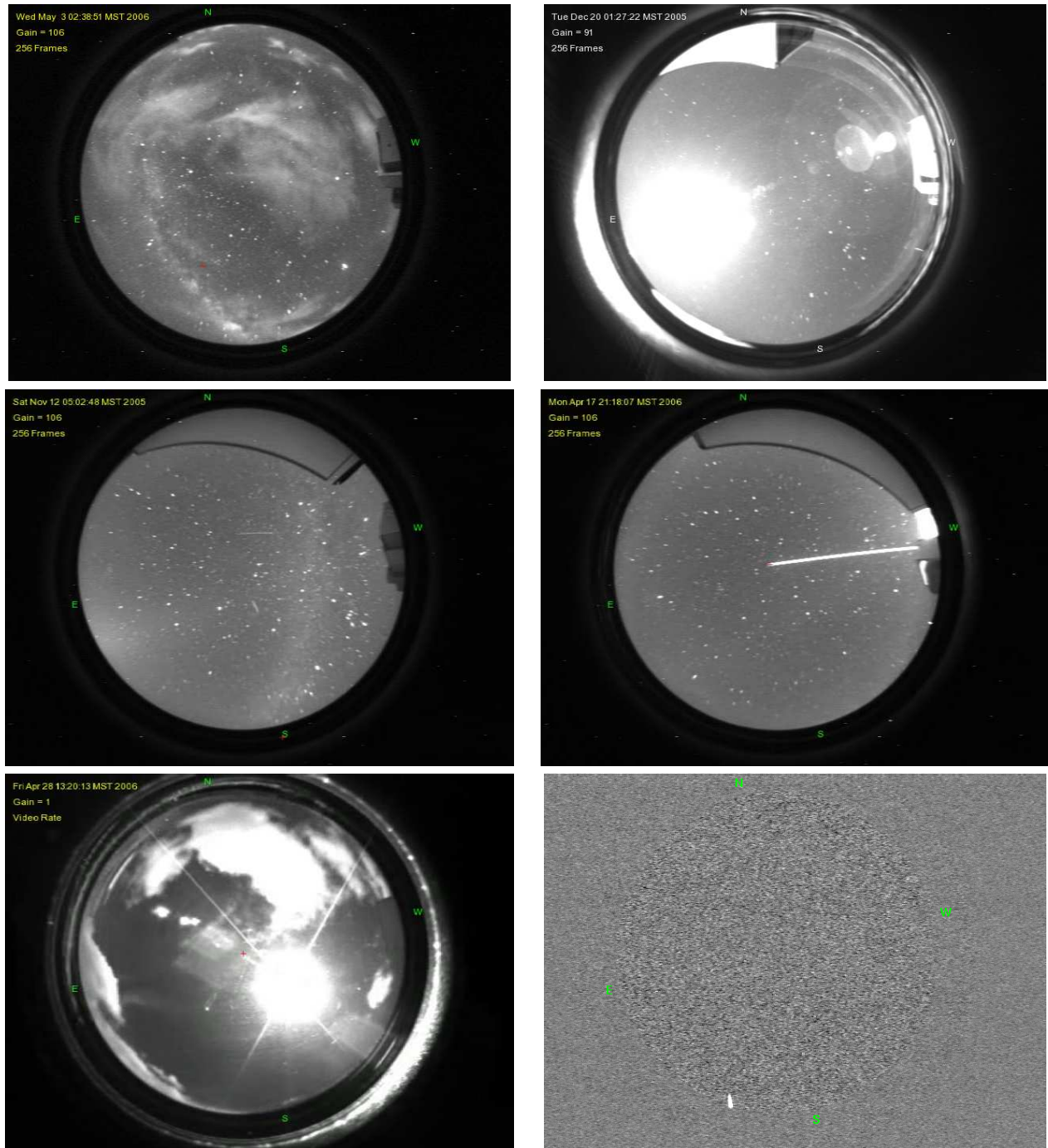


**Figure 4.** Selected images from the MMT All-Sky Camera. *Upper Left:* Dark night with scattered cirrus. The glow from the surrounding communities of Tucson and Nogales makes even very light cirrus plainly visible, especially when images are shown in animation. *Upper Right:* Bright night with a nearly full moon. There is a fair amount of scattering and internal reflection, but the image is still useful for detecting clouds. Orion and Canis Major are visible in the southwest and Ursa Major can be seen rising in the northeast. *Middle Left:* Image showing a couple of meteors and bright zodiacal light. *Middle Right:* Image showing our rayleigh laser AO system in operation. *Bottom Left:* Image taken during the day showing how the system performs under direct sunlight. *Bottom Right:* Example of a difference image between successive frames with a bright meteor low in the southeast.

differently and more slowly. This system has also proven to be an effective way to detect precipitation. The window provides enough collecting area to detect light sprinkles that might otherwise go unnoticed. This is an important safety consideration since conditions on Mt. Hopkins can change very rapidly and light rain can fall even when the humidity is not particularly high.

With a 10 second interval between images, the data rate of raw images is about 3 GB per day. Since we are not currently interested in archiving the data for quantitative purposes, we compress the images down and archive them into DivX format movies at sunrise and sunset every day. The resulting movies range from 12 to 20 MB in size which is about a factor of 100 in compression. Because the changes from frame to frame are usually small, these levels of compression can be obtained with a fairly high level of fidelity when using an advanced video codec. Comparing single frames from the DivX movies with the original images finds much of the detail intact with some smoothing of the background. The archived movies are made available at <http://skycam.mmta.arizona.edu/>.

## 5. CONCLUSIONS AND FUTURE WORK

After a full year of operation the MMT all-sky camera system has proven to be very successful as a cost-effective, robust way to monitor sky conditions. It provides frequently updated images of the whole sky down to an elevation of  $15^\circ$  at a sensitivity of at least that of a fully dark-adapted human eye. The ability to detect even small amounts of precipitation on the entrance window helps assure facility safety. Archiving the data in the form of reasonably-sized movie files makes it easy for observers to go back and check what the sky conditions were when their data was taken. We are working on integrating sky camera images into the data acquisition systems for our instruments to make this much easier and more direct.

The system was not initially designed with quantitative analysis of images in mind. For example, we selected the StellaCam II camera without knowing how stable or reproducible its gain values are. The 8-bit readout of the framegrabber is also far less desirable than a 16-bit direct CCD system. However, it appears that the StellaCam II is fairly stable and reproducible so that much more can be done in terms of photometric and sky brightness monitoring. We are now archiving difference images and are developing routines to automatically find and flag transient phenomena. In addition to finding meteors and satellites, this could be useful for automatically detecting aircraft while our laser AO system is in operation. We are also exploring ways to use difference images to quantify cloudiness.

## ACKNOWLEDGMENTS

I would like to express many thanks to Cory Knop, Ken van Horn, Phil Ritz, and the rest of the MMTO mountain staff for their hard work installing the all-sky camera system and keeping it maintained.

## REFERENCES

1. W. E. Pereira, "The CONCAM global sky monitoring network: Its evolution and the creation of a performance model," *Ph.D. Thesis*, 2003.
2. R. Smith, D. Walker, and H. E. Schwarz, "The Tololo All Sky Camera," in *Scientific Detectors for Astronomy, The Beginning of a New Era*, P. Amico, J. W. Beletic, and J. E. Beletic, eds., pp. 379–384, 2004.
3. J.-G. Cuby, P. Barriga, R. Cabanac, R. Castillo, I. Gavignaud, G. Gillet, N. Haddad, M. Kiekebusch, M. Marchesi, P. Mardones, M. Riquelme, P. Robert, and S. Rondi, "Instrumentation activities at Paranal Observatory," in *Observatory Operations to Optimize Scientific Return III. Edited by Quinn, Peter J. Proceedings of the SPIE, Volume 4844, pp. 35-45 (2002).*, P. J. Quinn, ed., pp. 35–45, Dec. 2002.
4. K. S. J. Anderson, J. Brinkmann, M. Carr, D. Woods, D. P. Finkbeiner, J. E. Gunn, C. L. Loomis, D. Schlegel, and S. Snedden, "Apache Point Observatory's All-Sky Camera: Observing Clouds in the Thermal Infrared," *Bulletin of the American Astronomical Society* **34**, pp. 1130–+, Dec. 2002.
5. W. Pence, "CFITSIO, v2.0: A New Full-Featured Data Interface," in *ASP Conf. Ser. 172: Astronomical Data Analysis Software and Systems VIII*, D. M. Mehringer, R. L. Plante, and D. A. Roberts, eds., pp. 487–+, 1999.